ANTIMICROBIAL AGENTS AND CHEMOTHERAPY, June 2005, p. 2172–2179 Vol. 49, No. 6
0066-4804/05/$08.00+0 doi:10.1128/AAC.49.6.2172–2179.2005

IMP Dehydrogenase from the Protozoan Parasite *Toxoplasma gondii*

William J. Sullivan, Jr.,[1] Stacy E. Dixon,[1] Catherine Li,[2] Boris Striepen,[2] and Sherry F. Queener[1]*

Department of Pharmacology and Toxicology, Indiana University School of Medicine, Indianapolis, IN 46202,[1] and Center for Tropical and Emerging Global Diseases and Department of Cellular Biology, University of Georgia, Athens, GA 30602[2]

Received 17 November 2004/Returned for modification 26 January 2005/Accepted 8 February 2005

The opportunistic apicomplexan parasite *Toxoplasma gondii* damages fetuses in utero and threatens immunocompromised individuals. The toxicity associated with standard antitoxoplasmal therapies, which target the folate pathway, underscores the importance of examining alternative pharmacological strategies. Parasitic protozoa cannot synthesize purines de novo; consequently, targeting purine salvage enzymes is a plausible pharmacological strategy. Several enzymes critical to purine metabolism have been studied in *T. gondii*, but IMP dehydrogenase (IMPDH), which catalyzes the conversion of IMP to XMP, has yet to be characterized. Thus, we have cloned the gene encoding this enzyme in *T. gondii*. Northern blot analysis shows that two IMPDH transcripts are present in *T. gondii* tachyzoites. The larger transcript contains an open reading frame of 1,656 nucleotides whose deduced protein sequence consists of 551 amino acids (TgIMPDH). The shorter transcript is an alternative splice product that generates a 371-amino-acid protein lacking the active-site flap (TgIMPDH-S). When TgIMPDH is expressed as a recombinant protein fused to a FLAG tag, the fusion protein localizes to the parasite cytoplasm. Immunoprecipitation with anti-FLAG was employed to purify recombinant TgIMPDH, which converts IMP to XMP as expected. Mycophenolic acid is an uncompetitive inhibitor relative to NAD^+, with a intercept inhibition constant (K_{ii}) of 0.03 ± 0.004 μM. Tiazofurin and its seleno analog were not inhibitory to the purified enzyme, but adenine dinucleotide analogs such as TAD and the nonhydrolyzable β-methylene derivatives of TAD or SAD were inhibitory, with K_{ii} values 13- to 60-fold higher than that of mycophenolic acid.

IMP dehydrogenase (IMPDH) converts IMP to XMP in the presence of NAD, a critical rate-limiting step in the biosynthesis of guanine nucleotides. Increased IMPDH activity is associated with actively dividing cells; consequently, IMPDH has been exploited as a target for anticancer, antiviral, immunosuppressive, and antimicrobial drug therapies (9, 15). Significant differences in IMDPH enzyme kinetics and inhibitor sensitivities between human and microbial homologues suggest that IMPDH may be an exploitable target for antimicrobials (25, 36, 40, 42). Purine metabolic enzymes hold particular promise as targets to combat intracellular parasites while minimizing side effects to host cells. Parasites are inherently more reliant on these enzymes to maintain growth and are incapable of synthesizing purine precursors de novo (34).

Toxoplasma gondii is an obligate intracellular protozoan responsible for fetal damage when the infection is acquired in utero (24), heart transplant complications (37), and opportunistic infections in immunocompromised individuals (39). *T. gondii*, as a member of the phylum Apicomplexa, is related to other parasites such as *Plasmodium* spp. (malaria) and *Cryptosporidium* spp. (26). A wide variety of molecular genetic tools have been developed for *T. gondii* (27, 28). In particular, the generation of reagents for reverse genetics has facilitated the study of the purine salvage network in this organism. Insertional mutagenesis has led to the cloning of *T. gondii* hypoxanthine-xanthine-guanine-phosphoribosyltransferase (HXGPRT), adenosine kinase (AK), and an adenosine transporter (TgAT) (3, 6, 32). Both biochemical studies (23, 29) and the generation of viable parasites lacking AK or HXGPRT demonstrate functional redundancy in pathways leading to GMP (2, 6, 32). Thus, drugs designed to inhibit only one route (via either AK and IMPDH or HXGPRT) would be ineffective. Thus, therapeutic exploitation of HXGPRT inhibitors depends upon simultaneous inhibition of GMP synthesis via the AK pathway. IMPDH is the logical target in the AK pathway both because of its regulatory significance and because of the wealth of inhibitors available. While IMPDHs have been cloned in other apicomplexans such as *Plasmodium* and *Cryptosporidium* spp. (14, 31), *T. gondii* IMPDH has not been available for study.

Here we describe the IMPDH gene in *T. gondii*, which gives rise to two transcripts, TgIMPDH and TgIMPDH-S. The latter is generated by an alternative splicing event that removes the active-site flap. Recombinant TgIMPDH was expressed and purified from *T. gondii* parasites for kinetic analysis. This full-length enzyme is inhibited by mycophenolic acid and adenine dinucleotide analogs, with intercept inhibition constant (K_{ii}) values in the micromolar to submicromolar range. The identification of this important purine interconversion enzyme constitutes a significant contribution to understanding purine salvage in *T. gondii*.

MATERIALS AND METHODS

Parasite culture and reagents. *T. gondii* tachyzoites (RH and RHΔHX strains) were cultured in primary human foreskin fibroblasts (HFF) in Dulbecco modified Eagle medium supplemented with 1% fetal bovine serum and gentamicin. Cultures were maintained in a humidified CO_2 (5%) incubator at 37°C. Total RNA was purified from filter-purified parasites using Trizol reagent (Invitrogen) and mRNA using the Poly(A)Pure system (Ambion), both followed by 1 h of incubation at 37°C with RQ1 DNase.

* Corresponding author. Mailing address: Department of Pharmacology and Toxicology, Medical Sciences Building Room A-519, Indiana University School of Medicine, 635 Barnhill Drive, Indianapolis, IN 46202-5120. Phone: (317) 274-1563. Fax: (317) 274-7714. E-mail: queenes@iupui.edu.

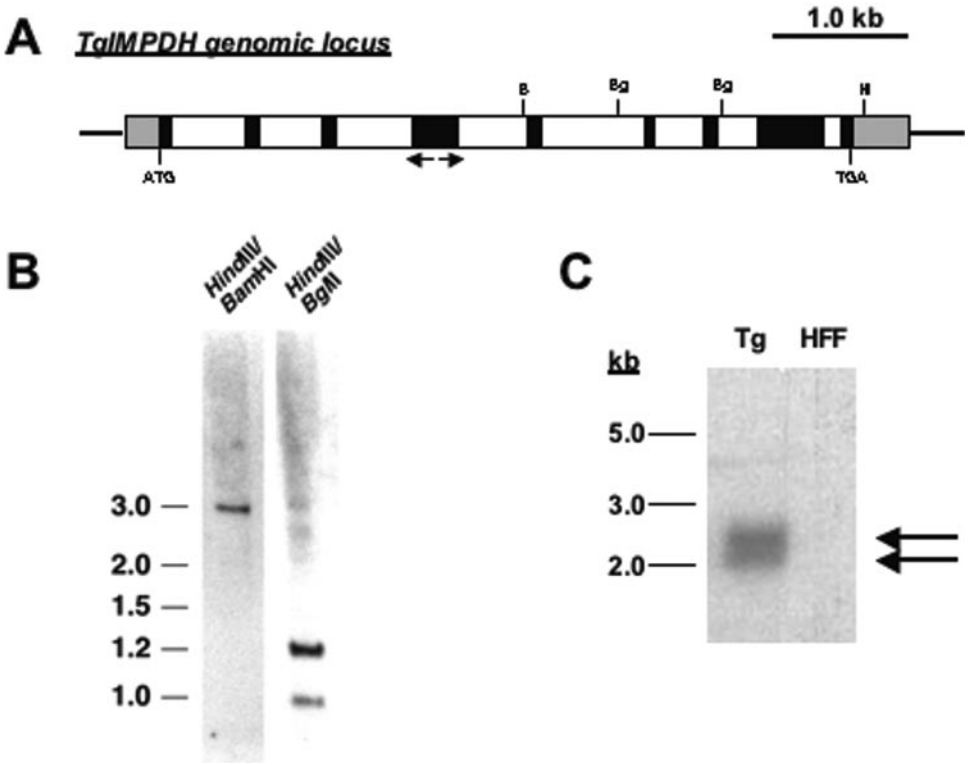

FIG. 1. *T. gondii* IMPDH gene. A. Schematic diagram of TgIMPDH locus. Gene-specific primers used for 5′- and 3′-RACE are designated by arrows. Black boxes denote exons, white boxes denote introns, and gray boxes denote untranslated regions. B, BamHI; Bg, BglII; H, HindIII. B. Southern blot analysis. Genomic DNA from *T. gondii* was digested with the indicated restriction enzymes and probed with labeled cDNA representing TgIMPDH. Numbers at left are sizes in kilobases. C. Northern analysis. Full-length cDNA representing the entire ~1.6-kb coding region of TgIMPDH was used to probe a Northern blot containing *T. gondii* mRNA (Tg) and host cell (HFF) total RNA.

RACE. 5′- and 3′ rapid amplification of cDNA end (RACE) reactions were performed with total RNA using GeneRacer (Invitrogen) and the following gene-specific primers, listed as "parent" and "nesting" oligonucleotides, respectively: for 3′-RACE, 5′-AGAAAGGGAAGCTCCCGATTGTGAACG and 5′-AGAGTTTCCACTCGCCTCGAAGGACTCC; for 5′-RACE, 5′-AGTCCTTCGAGGCGAGTGGAAACTCTCG and 5′-TCTTTGACTCCCGCAGCAGTTCGTTTGCC (Fig. 1A). Both 5′- and 3′-RACE PCRs utilized cDNA generated with the oligo(dT) primer included with the kit.

Bioinformatics and DNA sequencing. Preliminary genomic sequence data were accessed via http://ToxoDB.org (release 1.0) (21). Genomic data were provided by The Institute for Genomic Research (supported by the National Institutes of Health [NIH] grant no. AI05093) and by the Sanger Center (Wellcome Trust). BLAST analyses were run at http://www.ncbi.nih.gov/BLAST/, and multiple sequence alignments were produced using CLUSTALW (33). DNA sequencing was performed at the Biochemistry Biotechnology Facility (Indiana University School of Medicine, Indianapolis, IN).

Expression and purification of recombinant TgIMPDH. TgIMPDH was amplified from *T. gondii* total RNA using the SuperScript One-Step reverse transcription-PCR kit (Invitrogen) and the following primers, which generate restriction sites NdeI and AvrII for installation into a *T. gondii* expression vector that uses the *TUB* promoter and HXGPRT selection system (6): 5′-CATATGAAAATGGCTGACGGATGGGATGCGGAGAAAATC (sense) and 5′-CCTAGGGGCGTAGAGCTTTCTCTCGAAGCTGTGC (antisense). The TgIMPDH insert was fused in frame to a C-terminal FLAG (Sigma) tag, creating the vector designated *p*tubTgIMPDH$_{FLAG}$::HX. The nucleotide sequence of both strands of the insert was determined to confirm the fidelity of the PCR. Following electroporation, tachyzoites were selected in 25 μg/ml mycophenolic acid plus 50 μg/ml xanthine and cloned by limiting dilution (28). Clones were examined by immunofluorescence assay with anti-FLAG (Sigma) to select for those expressing recombinant tagged protein. For immunoprecipitation, ~10^9 freshly lysed tachyzoites were filtered-purified and harvested by centrifugation. Parasites were lysed by sonication in 1.0 ml of 50 mM Tris HCl (pH 7.4), 150 mM NaCl, 1 mM EDTA, and 1% Triton X-100 supplemented with a protease inhibitor cocktail (Sigma). The parasite lysate was clarified by centrifugation at 8,200 × *g* at 4°C for 10 min prior to mixing with 50 μl equilibrated anti-FLAG M2-agarose affinity gel. The affinity gel and lysate were mixed overnight at 4°C and spun at 8,200 × *g*. The supernatant (unbound fraction) was removed and stored for later analysis. The pelleted resin was washed three times in the lysis buffer above without the Triton X. 3× FLAG peptide was used to elute the material bound to the anti-FLAG resin for further analysis.

Immunofluorescence assays. Parasite clones expressing recombinant TgIMPDH$_{FLAG}$ were inoculated onto HFF monolayers grown on glass coverslips in 12-well tissue culture plates. Infected cell monolayers were fixed in methanol for 10 min at −20°C. After blocking in phosphate-buffered saline (PBS) containing 1% fish gelatin, 3% bovine serum albumin, and 5% goat serum for 1 h, mouse polyclonal anti-FLAG (Sigma) was applied at 1:250 (in PBS with 3% bovine serum albumin) for 1 h, followed by goat anti-rabbit Alexa 488 at 1:1,000 after PBS washes. 4′,6′-Diamidino-2-phenylindole (DAPI) nuclear stain was added for 5 min prior to visualization with a Leica DMLB microscope. Images were captured using a Spot RTSE model 12.0 monochrome camera and Spot Diagnostic Software version 3.5.9.

Enzymatic assays. IMPDH activity was measured using a fixed-time assay followed by thin-layer chromatography to separate radiolabeled substrate and products (12). The 50-μl reaction mixture contained 100 mM Tris-HCl buffer (pH 8.0), 100 mM KCl, 1 mM dithiothreitol, 3 mM EDTA, 2.3 mM NAD, 80 μM IMP, and 10 to 180 ng of purified protein. At the end of the 60-min incubation at 37°C, the reaction was quenched by adding 25 μl of carrier solution containing IMP, XMP, GMP, and hypoxanthine, each at a concentration of 4 mM. Ten-microliter samples of the reactions were spotted onto polyethyleneimine-cellulose plates that were prewashed with 100% methanol. The plates were developed in 0.5 M LiCl for 2 h. R_f values for the standards were as follows: XMP, 0.11; GMP, 0.32; IMP, 0.5; hypoxanthine, 0.86. Activity is expressed as concentration of product formed per minute, calculated from specific activity of the radiolabeled substrate. The assay is linear with protein concentration over the range used for all assays and has low variability; standard errors of the means typically averaged 3.2% of the means within assays and 4.7% from day to day.

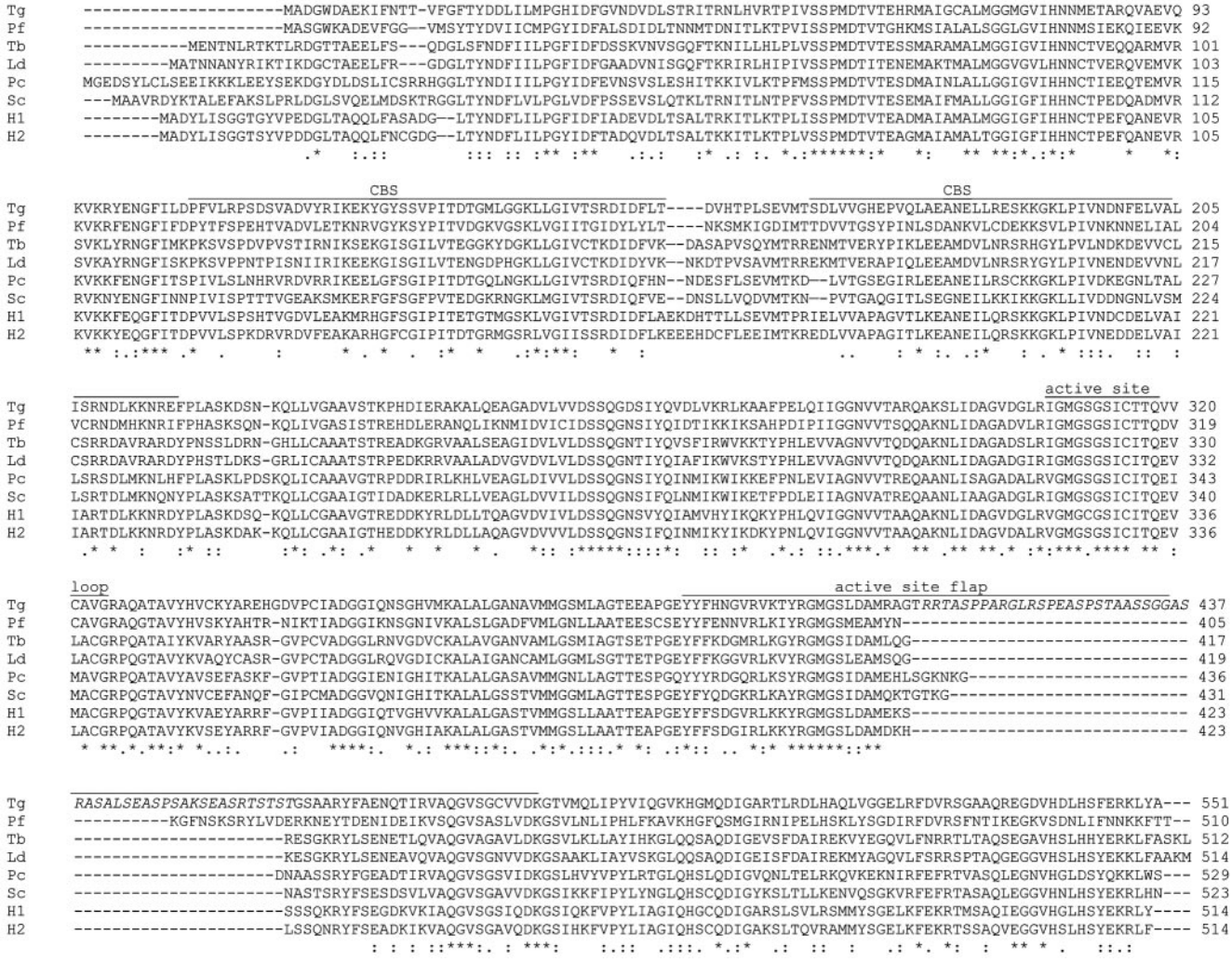

FIG. 2. IMPDH amino acid sequence alignments. Protein sequence alignments from various IMPDH homologues were compiled with CLUSTALW with manual adjustment. Tg, *Toxoplasma gondii*; Pf, *Plasmodium falciparum*; Tb, *Trypanosoma brucei*; Ld, *Leishmania donovani*; Pc, *Pneumocystis carinii*; Sc, *Saccharomyces cerevisiae*; H1 and H2, *Homo sapiens* isoforms 1 and 2, respectively. Indicated are the CBS domains as well as the active-site loop and flap. The atypical serine-rich insertion in TgIMPDH is shown in italics. Asterisks denote residues that are identical across these species. Colons represent conserved amino acid substitutions, while periods represent less conserved residue substitutions.

Curve fitting for kinetic experiments was done with Prism 3.0, using the standard equations for linear regressions and for the hyperbolic single-site curve. Ultimately, all experiments with various NAD^+ concentrations were evaluated with the equation entered for substrate inhibition, because NAD^+ at high concentrations inhibited the enzyme reaction: $v = V_{max}[NAD^+]/(K_m + [NAD^+] + [NAD^+]^2/K_i)$, where V_{max} is the maximal velocity of the reaction, K_m is the Michaelis constant, and K_i is the inhibition constant for NAD^+. Mycophenolic acid inhibition followed uncompetitive inhibition, according to the following equation: $v = V_{max}[NAD^+]/(K_{app} + [NAD^+][1 + [I]/K_{ii})$, where K_{app} is the apparent Michaelis constant for NAD^+ and K_{ii} is the intercept inhibition constant. The equation for uncompetitive inhibition was accepted when the results of four experiments showed that there was no statistical difference in the ratio of K_m/V_{max} in the uninhibited and the inhibited state. The equation for mixed noncompetitive inhibition was used to characterize inhibition by tiazofurin and its analogs. The equation is $v = V_{max}[NAD^+]/[K_m](1 + [I]/K_{is}) + [NAD^+](1 + [I]/K_{ii})$, where K_{is} is the slope inhibition constant and K_{ii} is the intercept inhibition constant.

Nucleotide sequence accession number. Nucleotide sequence data reported in this paper are available in the GenBank, EMBL, and DDBJ databases under the accession numbers AY661469 (TgIMPDH) and AY663109 (TgIMPDH-S).

RESULTS AND DISCUSSION

Identification of an IMPDH homologue in *T. gondii*. The *T. gondii* database was mined for sequences encoding IMPDH using the BLAST algorithm and text queries. Two contigs (Tgg_18808 and -18809) showing a high degree of similarity to nonoverlapping regions of human IMPDH were identified. Based on the sequence data, primers were designed to obtain the full-length cDNA employing 5′- and 3′-RACE. Using the primers listed in Materials and Methods, an 822-bp band representing the 5′ end of the gene and a 1,532-bp band representing the 3′ end were amplified and subcloned for sequencing. Considered with the genomic data, the predicted open reading frame is 1,656 bp, possessing 5′ and 3′ untranslated regions of 292 and 518 bp, respectively. The putative start codon fits Kozak consensus rules (22). There is no in-frame stop codon upstream of this proposed start site, but no other

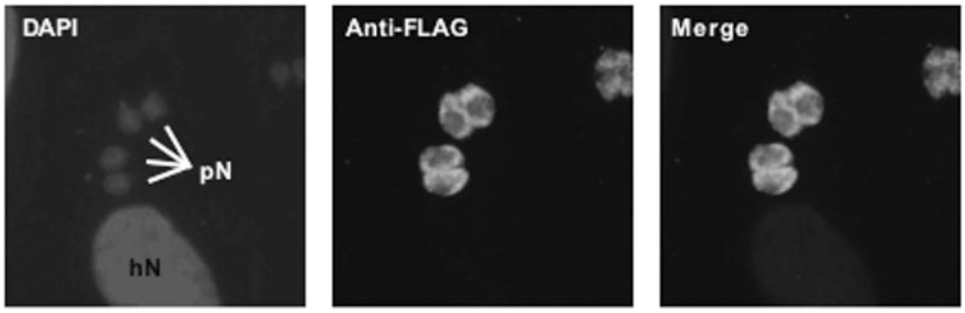

FIG. 3. Localization of recombinant TgIMPDH. Recombinant TgIMPDH containing a C-terminal FLAG-tag fusion localizes to the parasite cytoplasm. Parasites were costained with DAPI, which stains the nuclei of parasites (pN) and host cells (hN).

translation initiation sites exist downstream of the transcription start site determined by 5′-RACE.

Additional genomic sequences were procured from ToxoDB, allowing the construction of a hypothetical locus containing eight introns. A schematic diagram of the TgIMPDH genomic locus is shown in Fig. 1A, along with a Southern analysis consistent with a single-copy locus (Fig. 1B).

TgIMPDH cDNA hybridizes to two transcripts. Northern blot analysis used the full-length cDNA for TgIMPDH as a probe. Figure 1C shows hybridization to a ~2.5-kb band, consistent with our cloning results. However, an additional band at ~2.0 kb also hybridizes to the probe, suggesting another isoform of IMPDH is present in *T. gondii*. Since the ToxoDB and Southern analyses are consistent with the TgIMPDH locus being present as a single copy, we postulated that an alternatively spliced transcript may be present. Primers designed to amplify the IMPDH coding sequence from *T. gondii* total RNA produce the expected 1.6-kb band as well as a fainter 1.2-kb band. Each band was gel purified and sequenced. The 1.6-kb product agrees with our original open reading frame sequence prediction; the 1.2-kb product (referred to as TgIMPDH-S, for short form) lacks an internal 506-nucleotide region. The length of TgIMPDH-S including the untranslated regions is 2.0 kb, in agreement with the Northern analysis. TgIMPDH-S encodes a predicted 371-amino-acid form of IMPDH that lacks the active-site flap. The question of whether this shortened version of TgIMPDH possesses catalytic activity or perhaps serves some other regulatory function in the organism is intriguing. However, for these characterization studies we chose to use the longer form, which has more complete homology to other catalytically active IMPDH enzymes.

Comparison of TgIMPDH to other species. The deduced amino acid sequence of TgIMPDH is aligned, with salient domains identified, for comparison to IMPDH sequences from other species (Fig. 2). BLASTp analysis reveals that TgIMPDH is most similar to mammalian IMPDH (e.g., 53% identity to the human type II enzyme), followed by *Xenopus laevis* and the apicomplexan *Plasmodium yoelii* (50% identity). The IMPDH orthologue cloned from fellow apicomplexan *Cryptosporidium parvum* is only 35% identical, consistent with the observation that CpIMPDH was acquired through lateral gene transfer from bacteria (31).

The deduced secondary structure of TgIMPDH is similar to those of other known enzymes (11). The N-terminal and C-terminal regions are short elements at either end of the main structural feature of the molecule, the large barrel core. The barrel core is interrupted by three elements: a flanking region, an active-site loop, and an active-site flap. The flanking region has been noted in other species to interrupt the barrel core of the protein but does not interact with either substrate or cofactor in any crystal structures currently available. The flanking region in all IMPDH proteins studied contains two CBS (cystathionine beta-synthase) motifs; for TgIMPDH these motifs involve amino acid residues 105 to 156 and residues 168 to 216, making their position and length nearly identical to those of the CBS motifs in human type II IMPDH. The active-site loop

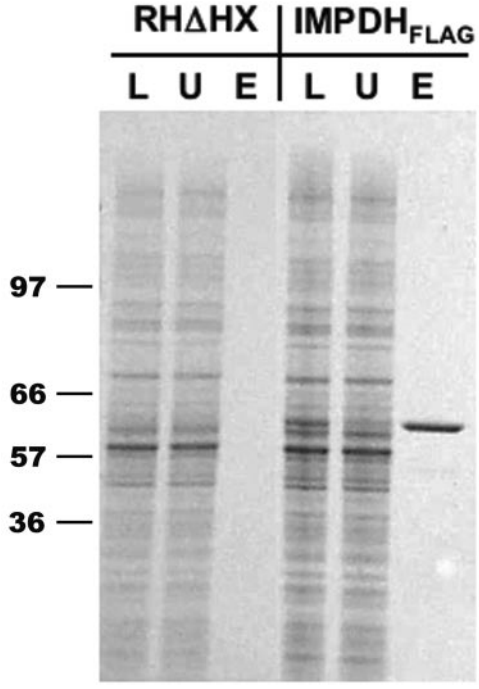

FIG. 4. Expression and purification of recombinant TgIMPDH. Transgenic parasite clones stably expressing recombinant $TgIMPDH_{FLAG}$ were selected in mycophenolic acid and xanthine following the electroporation of plasmid into RHΔHX parasites. TgIMPDH was purified by FLAG-based affinity chromatography and eluted from the resin with 3× FLAG peptide. Lysate (L), the unbound fraction (U), and the eluate (E) were resolved by sodium dodecyl sulfate-polyacrylamide gel electrophoresis, and proteins were visualized by SimplyBlue stain. Molecular mass markers are shown in kilodaltons.

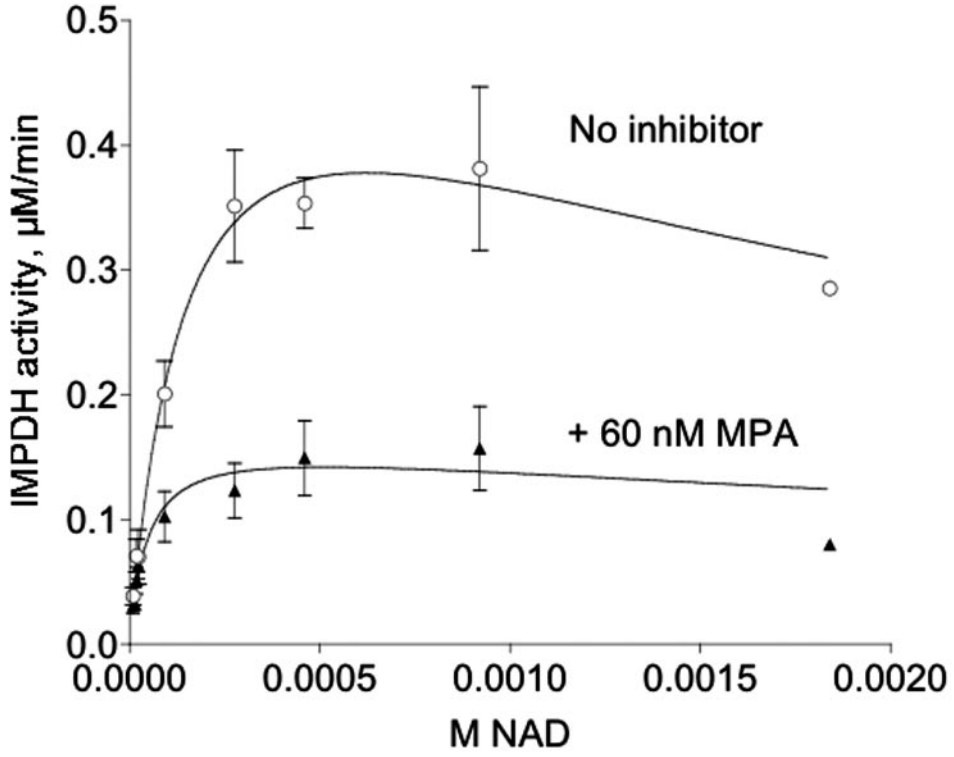

FIG. 5. Mycophenolic acid inhibition of recombinant TgIMPDH. The dependence of the enzymatic reaction on NAD^+ was assessed for purified recombinant $TgIMPDH_{FLAG}$ with and without a fixed concentration of mycophenolic acid (MPA). Results from four independent experiments were combined; means with error bars representing the standard errors of the means are shown. Data were fitted to the equation describing substrate inhibition, since high concentrations of NAD^+ were inhibitory (see Materials and Methods). Nonlinear regression (Prism 3.0) was used to calculate V_{max} and K_m values for both curves. The V_{max} values (means ± standard errors of the means) are 0.570 ± 0.16 and 0.168 ± 0.04 μM/min for the top and bottom curves, respectively; the K_m values are 158.1 ± 86.7 and 46.7 ± 25.7 μM for the top and bottom curves, respectively.

of the *T. gondii* enzyme is highly conserved with other species but not identical, as discussed below. The most striking difference in structure is in the active-site flap, a flexible element that closes over the active site when cofactor and substrate are bound. TgIMPDH contains a unique 50-amino-acid insertion (residues 410 to 460, *T. gondii* numbering) that is rich in serine and proline (Fig. 2). This unique insertion is in the disordered portion of the flap region. The physiological relevance of this insertion in the *T. gondii* enzyme remains to be determined.

Data from published crystal structures of human type II, hamster, *Tritrichomonas foetus*, and *Streptococcus pyogenes* IMPDHs allow a more detailed comparison of the potential critical differences between the sequence of TgIMPDH and other forms. As expected, key catalytic residues such as Cys331 (human enzyme numbering), which carries out the nucleophilic attack on the C-2 position of the inosine ring, are conserved in both *T. gondii* and *Plasmodium falciparum* IMPDH. Other residues in the active-site loop (amino acids 325 to 340 for the human enzyme) such as Gly326, Thr333, and Ser329, which interact with substrate or cofactor in existing crystal structures (10, 30, 41), are also conserved in the apicomplexan enzymes.

Two residues within the active-site loop differ between the human and the *T. gondii* enzyme. The conserved isoleucine present at position 332 of the human enzymes is replaced by a threonine residue in both the *T. gondii* and *P. falciparum* enzymes. Likewise, a conserved glutamic acid at position 335 in the human enzyme is replaced by a valine in the *T. gondii* enzyme and an aspartic acid in the *P. falciparum* enzyme. The impact of these substitutions needs to be explored.

The IMP binding site involves residues outside the active-site loop, as shown by crystal structures for several enzymes (11), and these residues are generally conserved in TgIMPDH. In the enzymes studied by crystal structure, Gly366, Gly387, Ser388, and Tyr411 stabilize the phosphate group of IMP into the active site. These residues are conserved in TgIMPDH. The ribose of IMP interacts with Ser68 and Asp364 of the human enzyme. These residues are conserved in the apicomplexan enzymes. Likewise, residues Met414, Gly415, and Gln441, which interact with the inosine ring in the human enzyme, are conserved in the apicomplexan enzymes.

The NAD binding cleft has been probed with crystal structures for hamster, human, and *T. foetus* IMPDH (11). Polar interactions of the carboxamide group of nicotinamide exist with Asn303, Arg322, and Asp274, residues that are conserved in the apicomplexan enzymes. Mycophenolic acid interacts with these same residues. Mycophenolic acid has additional interactions in the human enzyme with Gly326, Thr333, and Gln441, which are conserved in the apicomplexan forms. The ribose phosphate portion of NAD interacts with Asp274, Ser275, and Ser276; these three amino acids are conserved in all species so far studied.

Residues from the adjacent monomers in the active tetramer interact with the ribose of NAD. Gln469, which is conserved

TABLE 1. Kinetics of TgIMPDH-F compared to those of the enzyme from other organisms[a]

Kinetic parameter	Protozoa				Fungi (*P. carinii*)[h]	Human		Bacteria	
	Apicomplexa			Other (*T. foetus*)[e]					
	T. gondii[b]	*C. parvum*[c]	*E. tenella*[d]			Type I[i]	Type II[j]	*E. coli*[k]	*B. burgdorferi*[m]
k_{cat} (s^{-1})	0.98 ± 0.05	3.3 ± 0.2		1.9 ± 0.2	0.56 ± 0.04	1.82 ± 0.04	0.39 ± 0.01 1.4 ± 0.04[i]	13 ± 1	2.6 ± 0.3
K_m of NAD (μM)	144 ± 12	150 ± 20	150	150 ± 30	24.4 ± 1.3	42 ± 6	6.0 ± 1.0 32 ± 3.6[i]	2,000 ± 500	1,100 ± 160
K_i of NAD (mM)	4.5 ± 1.2	2.9 ± 0.7	2.0	6.8 ± 1.8	2.6 ± 0.07		0.59 ± 0.02	2.8 ± 0.8	2.3 ± 0.4
k_{cat}/K_m ($mM^{-1} \cdot s^{-1}$)	6.8 ± 4	15 ± 3		13	23 ± 6	43	65 ± 0.5	6.5	2.4 ± 0.5
K_{ii} of MPA[p] (μM)	0.030 ± 0.004	9.3 ± 0.3	0.18	9.0 ± 0.5[f] 14.0 ± 2.0[g]	0.06 ± 0.003	0.011	0.006 0.022 ± 0.008[f]	20[f]	6 ± 1
K_{ii} of tiazofurin (μM)	>100	1,500 ± 100		69,000 ± 9,000[g]			1,300 ± 100[f]		
K_{ii} of Se-tiazofurin (μM)	>100								
K_{ii} of TAD (μM)	1.77 ± 0.73			1.6 ± 0.2[g]		0.71[n]	0.43[n]	8.5[l]	
K_{ii} of SAD (μM)						0.06[o]	0.03[o]		
K_{ii} of CH_2-TAD (μM)	0.98 ± 0.45	0.6 ± 0.04		2.3 ± 0.4[f]		0.095	0.06 ± 0.02[f] 0.145[i]		1 ± 1
K_{ii} of CH_2-SAD (μM)	0.38 ± 0.05								

[a] All data within the columns come from the reference denoted in the column header, unless otherwise specified by a footnote to the value. The data for the *T. gondii* enzyme are means ± standard errors of the means calculated from *n* independent experiments. $n = 3$ for k_{cat}, K_m of NAD, and K_{ii} of TAD; 10 for K_i of NAD; 8 for K_{ii} of mycophenolic acid; and 2 for K_{ii} of CH_2-TAD and CH_2-SAD.
[b] Assays at 37°C using the thin-layer chromatography assay described in Materials and Methods: 460 μM NAD, 80 μM IMP.
[c] Reference 35. Assays at 25°C. Spectrophotometric assay: 500 μM NAD, 250 μM IMP.
[d] Reference 17. Assays at 37°C. Thin-layer chromatography assay: 500 μM NAD, 30 μM IMP.
[e] Reference 5. Assays at 25°C. Spectrophotometric assay: 1,000 μM NAD, 100 μM IMP.
[f] Reference 4. Assays at 25°C. Spectrophotometric assay: 400 μM NAD, 150 μM IMP.
[g] Reference 16. Assays at 25°C. Spectrophotometric assay: 1,000 μM NAD, 200 μM IMP.
[h] S.F. Queener and D.J. Ye, unpublished. Assays at 25°C. Spectrophotometric assay: 250 μM NAD, 180 μM IMP.
[i] Reference 13. Assays at 37°C. Spectrophotometric assay: not defined.
[j] Reference 38. Assays at 25°C. Spectrophotometric assay: 40 to 800 μM NAD, 250 μM IMP.
[k] Reference 19. Assays at 25°C. Spectrophotometric assay: 2,500 to 8,000 μM NAD, 750 to 1,000 μM IMP.
[l] Reference 20. Assays at 25°C. Spectrophotometric assay: 2,500 μM NAD, 1,000 μM IMP.
[m] Reference 42. Assays at 25°C. Spectrophotometric assay: 500 μM NAD, 250 μM IMP.
[n] Reference 8. Assays at 37°C. Spectrophotometric assay: 100 μM NAD, 100 μM IMP.
[o] Reference 18. Assays at 37°C. Thin-layer chromatography assay: 1,000 μM NAD, 286 μM IMP.
[p] MPA, mycophenolic acid.

between human and apicomplexan IMPDH, is one of these residues. Another is Ala46 in the human enzyme. Considerable variability exists at this site; the *T. gondii* and *Pneumocystis carinii* enzymes contain a valine, but the *P. falciparum* enzyme contains a leucine.

The highest degree of species variability in the NAD binding site occurs in the portion that interacts with the adenine ring. In the human enzyme Phe282 forms part of this interaction, but this residue is replaced by tyrosine in several species, including the apicomplexan enzymes. Another interaction in the human enzyme is with His253, which is replaced by a lysine in the *T. gondii* enzyme and by an arginine in the *P. falciparum* enzyme. Thr45 on an adjacent monomer contributes to binding the adenine ring in the human enzyme, but this residue is a glycine in TgIMPDH and an alanine in the *P. falciparum* enzyme.

Another important contributor to the enzymatic reaction is a bound water molecule and a bound potassium ion (1, 11). Binding involves the conserved Cys331, Gly328, and Gly326 residues in the active-site loop, as well as three residues near the C terminus: Glu500, Gly501, and Gly502. Both Glu500 and Gly501 are conserved between human and apicomplexan enzymes, but Gly502 is replaced by an aspartic acid in the *T. gondii* enzyme and a lysine in the *P. falciparum* enzyme. Since the water molecule and the potassium ion are known to play key catalytic roles in other IMPDH forms, the effects of these substitutions on activity should be explored.

Localization and enzymatic analysis of recombinant TgIMPDH. Numerous attempts to express functional recombinant TgIMPDH in a variety of bacterial systems failed, most likely due to lack of solubility of the recombinant protein. Therefore, we attempted expression in *T. gondii* itself and used a C-terminal FLAG epitope tag to purify TgIMPDH for analysis (7). The FLAG tag also allowed us to determine the subcellular localization of the recombinant enzyme. As expected, transgenic parasites transfected with *p*tubTgIMPDH$_{FLAG}$::HX (see Materials and Methods) exhibited a staining pattern suggesting that TgIMPDH is diffuse throughout the parasite cytoplasm (Fig. 3). Untransfected RHΔHX parasites do not exhibit fluorescence when analyzed in the same manner with anti-FLAG (data not shown). An anti-FLAG affinity resin was used to purify recombinant enzyme from a stably transfected parasite clone. Purified enzyme from the transgenic clone (RHΔHX::TgIMPDH$_{FLAG}$) was examined by staining sodium dodecyl sulfate-polyacrylamide gels with a Coomassie blue-based reagent. Parasites transfected with *p*tubTgIMPDH$_{FLAG}$::HX displayed a single band at the expected size (~60 kDa) following elution from the affinity matrix (Fig. 4).

To test enzymatic activity of TgIMPDH, the conversion of radiolabeled IMP to XMP was measured directly by thin-layer chromatography. Lysates from parental RHΔHX *T. gondii* served as negative controls to ensure that no endogenous IMPDH activity could be detected following FLAG purification. Protein-dependent conversion of IMP to XMP could

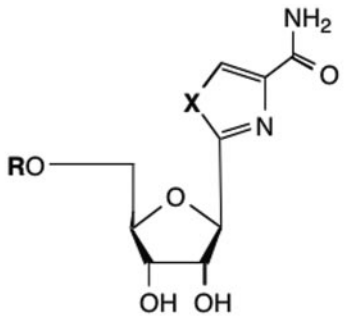

R	X	
H	S	Tiazofurin
H	Se	4-Selenazolecarboxamide (Se-tiazofurin)
$PO_3HPO_3HCH_2$-Adenosine	S	TAD
$PO_2HCH_2PO_3HCH_2$-Adenosine	S	β-Methylene TAD (CH_2TAD)
$PO_2HCH_2PO_3HCH_2$-Adenosine	Se	β-Methylene SAD

FIG. 6. Analogues of tiazofurin. All compounds were obtained from the Drug Development and Clinical Sciences Branch of the National Institute of Allergy and Infectious Diseases (Mohamed Nasr). A commercial preparation of tiazofurin was also tested. Tiazofurin is 2-β-D-ribofuranosylthiazole-4-carboxamide; Se-tiazofurin is 2-β-D-ribofuranosylselenazole-4-carboxamide; TAD is thiazole-4-carboxamide adenine dinucleotide; β-methylene TAD is 4-carboxamido-2-β-D-ribofuranosylthiazolyl adenosine methylenediphosphonic acid; β-methylene SAD is 4-carboxamido-2-β-D-ribofuranosylselenazolyl (5′ + 5′) adenosine methylenediphosphonic acid.

be achieved using $TgIMPDH_{FLAG}$ protein purified from the RHΔHX::$TgIMPDH_{FLAG}$ clone; assays using the eluted protein from untransfected RHΔHX parasites showed <0.2% of rates seen with recombinant protein. We therefore set out to characterize the catalytically active recombinant protein in terms of NAD^+ kinetics and sensitivity to an array of inhibitors.

$TgIMPDH_{FLAG}$ is sensitive to mycophenolic acid, a known inhibitor of other forms of IMPDH. Increasing amounts of mycophenolic acid in the assay produced classic sigmoidal inhibition curves (data not shown). Experiments assessing the effect of fixed concentrations of mycophenolic acid on NAD^+ dependence curves showed that inhibition by mycophenolic acid is uncompetitive (Fig. 5); as expected for uncompetitive inhibition, the ratio of the uninhibited to inhibited K_m value was equal to the ratio of the uninhibited to the inhibited V_{max} value, 3.385 and 3.393, respectively. These experiments allowed the calculation of a K_i value of 0.030 ± 0.004 μM (Table 1). $TgIMPDH_{FLAG}$ is therefore similar in sensitivity to IMPDH from another apicomplexan, *Eimeria tenella*, which has a K_i of 0.18 μM (17). *Cryptosporidium* IMPDH was acquired through lateral transfer from eubacteria, and predictably the sensitivity to mycophenolic acid differs from that of $TgIMPDH_{FLAG}$ (35). Both human forms of IMPDH and full-length IMPDH from *Pneumocystis* have K_i values in the submicromolar range, similar to $TgIMPDH_{FLAG}$. Bacterial forms of IMPDH are significantly less sensitive to mycophenolic acid than is $TgIMPDH_{FLAG}$.

Compounds known to inhibit mammalian forms of IMPDH were tested for their ability to inhibit $TgIMPDH_{FLAG}$ (Fig. 6). Like other IMPDH enzymes, $TgIMPDH_{FLAG}$ is poorly inhibited by tiazofurin or Se-tiazofurin (Table 1). The stronger inhibition by TAD and the nonhydrolyzable beta-methylene derivatives of TAD (CH_2-TAD) and SAD (CH_2-SAD) followed a mixed noncompetitive pattern with slightly more effect on V_{max} than K_m. The K_i values calculated from the equation for mixed noncompetitive inhibition (Table 1) show that $TgIMPDH_{FLAG}$ is most potently inhibited by CH_2-SAD, followed by CH_2-TAD and TAD. SAD was previously found to be a more potent inhibitor of both type I and type II human IMPDH than was TAD (8).

ACKNOWLEDGMENTS

We thank Pamela Torkelson for developing and performing the IMPDH assays, Micah M. Bhatti for the generation and immunofluorescence analysis of parasites expressing $TgIMPDH_{FLAG}$, and Jeramy Spurgeon for technical assistance with graphics. Preliminary genomic sequence data were accessed via http://ToxoDB.org (release 1.0).

Genomic data were provided by The Institute for Genomic Research (supported by NIH grant AI05093) and by the Sanger Center (Wellcome Trust). This work was funded by NIH AI-42024 (S.F.Q.) and NIH AI48475 and AI55268 and by further support from Merck Research Laboratories (B.S.).

REFERENCES

1. **Boritzki, T. J., D. A. Berry, J. A. Besserer, P. D. Cook, D. W. Fry, W. R. Leopold, and R. C. Jackson.** 1985. Biochemical and antitumor activity of tiazofurin and its selenium analog (2-beta-D-ribofuranosyl-4-selenazolecarboxamide). Biochem. Pharmacol. **34:**1109–1114.
2. **Chaudhary, K., J. A. Darling, L. M. Fohl, W. J. Sullivan, Jr., R. G. Donald, E. R. Pfefferkorn, B. Ullman, and D. S. Roos.** 2004. Purine salvage pathways in the apicomplexan parasite *Toxoplasma gondii*. J. Biol. Chem. **279:**31221–31227.
3. **Chiang, C. W., N. Carter, W. J. Sullivan, Jr., R. G. Donald, D. S. Roos, F. N. Naguib, M. H. el Kouni, B. Ullman, and C. M. Wilson.** 1999. The adenosine transporter of *Toxoplasma gondii.* Identification by insertional mutagenesis, cloning, and recombinant expression. J. Biol. Chem. **274:**35255–35261.
4. **Digits, J. A., and L. Hedstrom.** 2000. Drug selectivity is determined by coupling across the NAD^+ site of IMP dehydrogenase. Biochemistry **39:** 1771–1777.
5. **Digits, J. A., and L. Hedstrom.** 1999. Kinetic mechanism of *Tritrichomonas foetus* inosine 5′-monophosphate dehydrogenase. Biochemistry **38:**2295–2306.
6. **Donald, R. G., D. Carter, B. Ullman, and D. S. Roos.** 1996. Insertional tagging, cloning, and expression of the *Toxoplasma gondii* hypoxanthine-xanthine-guanine phosphoribosyltransferase gene. Use as a selectable marker for stable transformation. J. Biol. Chem. **271:**14010–14019.
7. **Donald, R. G., and P. A. Liberator.** 2002. Molecular characterization of a coccidian parasite cGMP dependent protein kinase. Mol. Biochem. Parasitol. **120:**165–175.
8. **Franchetti, P., L. Cappellacci, P. Perlini, H. N. Jayaram, A. Butler, B. P. Schneider, F. R. Collart, E. Huberman, and M. Grifantini.** 1998. Isosteric analogues of nicotinamide adenine dinucleotide derived from furanfurin, thiophenfurin, and selenophenfurin as mammalian inosine monophosphate dehydrogenase (type I and II) inhibitors. J. Med. Chem. **41:**1702–1707.
9. **Franchetti, P., and M. Grifantini.** 1999. Nucleoside and non-nucleoside IMP dehydrogenase inhibitors as antitumor and antiviral agents. Curr. Med. Chem. **6:**599–614.
10. **Gan, L., G. A. Petsko, and L. Hedstrom.** 2002. Crystal structure of a ternary complex of *Tritrichomonas foetus* inosine 5′-monophosphate dehydrogenase: NAD^+ orients the active site loop for catalysis. Biochemistry **41:**13309–13317.
11. **Goldstein, B., D. Risal, and M. Strickler.** 2003. IMPDH structure and ligand binding. ACS Symp. Ser. **839:**140–168.
12. **Gu, J. J., A. K. Tolin, J. Jain, H. Huang, L. Santiago, and B. S. Mitchell.** 2003. Targeted disruption of the inosine 5′-monophosphate dehydrogenase type I gene in mice. Mol. Cell. Biol. **23:**6702–6712.
13. **Hager, P. W., F. R. Collart, E. Huberman, and B. S. Mitchell.** 1995. Recombinant human inosine monophosphate dehydrogenase type I and type II

proteins. Purification and characterization of inhibitor binding. Biochem. Pharmacol. **49:**1323–1329.
14. **Hariharan, J., R. Rane, K. Ayyanathan, Philomena, V. P. Kumar, D. Prahlad, and S. Datta.** 1999. Mechanism-based inhibitors: development of a high throughput coupled enzyme assay to screen for novel antimalarials. J. Biomol. Screen. **4:**187–192.
15. **Hedstrom, L.** 1999. IMP dehydrogenase: mechanism of action and inhibition. Curr. Med. Chem. **6:**545–560.
16. **Hedstrom, L., and C. C. Wang.** 1990. Mycophenolic acid and thiazole adenine dinucleotide inhibition of *Tritrichomonas foetus* inosine 5′-monophosphate dehydrogenase: implications on enzyme mechanism. Biochemistry **29:** 849–854.
17. **Hupe, D. J., B. A. Azzolina, and N. D. Behrens.** 1986. IMP dehydrogenase from the intracellular parasitic protozoan *Eimeria tenella* and its inhibition by mycophenolic acid. J. Biol. Chem. **261:**8363–8369.
18. **Jayaram, H. N., J. A. Yalowitz, G. Krupitza, T. Szekeres, K. Krohn, and K. W. Pankiewicz.** 2003. Studies with benzamide riboside, a recent inhibitor of inosine 5′-monophosphate dehydrogenase. ACS Symp. Ser. **839:**231–246.
19. **Kerr, K. M., J. A. Digits, N. Kuperwasser, and L. Hedstrom.** 2000. Asp338 controls hydride transfer in *Escherichia coli* IMP dehydrogenase. Biochemistry **39:**9804–9810.
20. **Kerr, K. M., and L. Hedstrom.** 1997. The roles of conserved carboxylate residues in IMP dehydrogenase and identification of a transition state analog. Biochemistry **36:**13365–13373.
21. **Kissinger, J. C., B. Gajria, L. Li, I. T. Paulsen, and D. S. Roos.** 2003. ToxoDB: accessing the *Toxoplasma gondii* genome. Nucleic Acids Res. **31:** 234–236.
22. **Kozak, M.** 1991. Structural features in eukaryotic mRNAs that modulate the initiation of translation. J. Biol. Chem. **263:**19867–19870.
23. **Krug, E. C., J. J. Marr, and R. L. Berens.** 1989. Purine metabolism in *Toxoplasma gondii*. J. Biol. Chem. **264:**10601–10607.
24. **Martin, S.** 2001. Congenital toxoplasmosis. Neonatal Netw. **20:**23–30.
25. **O'Gara, M. J., C. H. Lee, G. A. Weinberg, J. M. Nott, and S. F. Queener.** 1997. IMP dehydrogenase from *Pneumocystis carinii* as a potential drug target. Antimicrob. Agents Chemother. **41:**40–48.
26. **Roos, D. S., M. J. Crawford, R. G. Donald, L. M. Fohl, K. M. Hager, J. C. Kissinger, M. G. Reynolds, B. Striepen, and W. J. Sullivan, Jr.** 1999. Transport and trafficking: *Toxoplasma* as a model for *Plasmodium*. Novartis Found. Symp. **226:**176–195.
27. **Roos, D. S., R. G. Donald, N. S. Morrissette, and A. L. Moulton.** 1994. Molecular tools for genetic dissection of the protozoan parasite *Toxoplasma gondii*. Methods Cell Biol. **45:**27–63.
28. **Roos, D. S., W. J. Sullivan, B. Striepen, W. Bohne, and R. G. Donald.** 1997. Tagging genes and trapping promoters in *Toxoplasma gondii* by insertional mutagenesis. Methods **13:**112–122.
29. **Schwartzman, J. D., and E. R. Pfefferkorn.** 1982. *Toxoplasma gondii*: purine synthesis and salvage in mutant host cells and parasites. Exp. Parasitol. **53:** 77–86.
30. **Sintchak, M. D., M. A. Fleming, O. Futer, S. A. Raybuck, S. P. Chambers, P. R. Caron, M. A. Murcko, and K. P. Wilson.** 1996. Structure and mechanism of inosine monophosphate dehydrogenase in complex with the immunosuppressant mycophenolic acid. Cell **85:**921–930.
31. **Striepen, B., M. W. White, C. Li, M. N. Guerini, S. B. Malik, J. M. Logsdon, Jr., C. Liu, and M. S. Abrahamsen.** 2002. Genetic complementation in apicomplexan parasites. Proc. Natl. Acad. Sci. USA **99:**6304–6309.
32. **Sullivan, W. J., Jr., C. W. Chiang, C. M. Wilson, F. N. Naguib, M. H. el Kouni, R. G. Donald, and D. S. Roos.** 1999. Insertional tagging of at least two loci associated with resistance to adenine arabinoside in *Toxoplasma gondii*, and cloning of the adenosine kinase locus. Mol. Biochem. Parasitol. **103:** 1–14.
33. **Thompson, J. D., D. G. Higgins, and T. J. Gibson.** 1994. CLUSTAL W: improving the sensitivity of progressive multiple sequence alignment through sequence weighting, position-specific gap penalties and weight matrix choice. Nucleic Acids Res. **22:**4673–4680.
34. **Ullman, B., and D. Carter.** 1995. Hypoxanthine-guanine phosphoribosyltransferase as a therapeutic target in protozoal infections. Infect. Agents Dis. **4:**29–40.
35. **Umejiego, N. N., C. Li, T. Riera, L. Hedstrom, and B. Striepen.** 2004. *Cryptosporidium parvum* IMP dehydrogenase: identification of functional, structural, and dynamic properties that can be exploited for drug design. J. Biol. Chem. **279:**40320–40327.
36. **Verham, R., T. D. Meek, L. Hedstrom, and C. C. Wang.** 1987. Purification, characterization, and kinetic analysis of inosine 5′-monophosphate dehydrogenase of *Tritrichomonas foetus*. Mol. Biochem. Parasitol. **24:**1–12.
37. **Wagner, F. M., H. Reichenspurner, P. Uberfuhr, M. Weiss, V. Fingerle, and B. Reichart.** 1994. Toxoplasmosis after heart transplantation: diagnosis by endomyocardial biopsy. J. Heart Lung Transplant. **13:**916–918.
38. **Wang, W., and L. Hedstrom.** 1997. Kinetic mechanism of human inosine 5′-monophosphate dehydrogenase type II: random addition of substrates and ordered release of products. Biochemistry **36:**8479–8483.
39. **Wong, S. Y., and J. S. Remington.** 1993. Biology of *Toxoplasma gondii*. AIDS **7:**299–316.
40. **Zhang, R., G. Evans, F. Rotella, E. Westbrook, E. Huberman, A. Joachimiak, and F. R. Collart.** 1999. Differential signatures of bacterial and mammalian IMP dehydrogenase enzymes. Curr. Med. Chem. **6:**537–543.
41. **Zhang, R., G. Evans, F. J. Rotella, E. M. Westbrook, D. Beno, E. Huberman, A. Joachimiak, and F. R. Collart.** 1999. Characteristics and crystal structure of bacterial inosine-5′-monophosphate dehydrogenase. Biochemistry **38:** 4691–4700.
42. **Zhou, X., M. Cahoon, P. Rosa, and L. Hedstrom.** 1997. Expression, purification, and characterization of inosine 5′-monophosphate dehydrogenase from *Borrelia burgdorferi*. J. Biol. Chem. **272:**21977–21981.